

Drug and chemical glucosidation by control SupersomesTM and membranes from *Spodoptera frugiperda* (Sf) 9 cells: Implications for the apparent glucuronidation of xenobiotics by UDP-glucuronosyltransferase 1A5

Nuy Chau¹, Leyla Kaya¹, Benjamin C. Lewis^{1,2}, Peter I. Mackenzie^{1,2} and John O. Miners^{1,2}

¹Department of Clinical Pharmacology, Flinders University College of Medicine and Public Health, Adelaide, Australia.

²Flinders Centre for Innovation in Cancer, Flinders University College of Medicine and Public Health, Adelaide, Australia.

Running title: Drug and chemical glucosidation by insect cell lines

Address for correspondence:

Professor John O. Miners

Department of Clinical Pharmacology

College of Medicine and Public Health

Flinders University

GPO Box 2100

Adelaide, SA 5001

Australia

Telephone: 61-401132104

Fax: 61-8-82045114

Email: john.miners@flinders.edu.au

Number of text pages: 34 (excluding Table)

Number of Figures: 4

Number of Tables: 1

Number of references: 36

Word counts:

Abstract – 248 words

Introduction – 705 words

Discussion – 1498 words

Abbreviations: AZT, zidovudine; BZC, benzocaine; COD, codeine; c-SUP, control SupersomesTM; HEK293T, human embryonic kidney 293T cell line; 21-OHPr, 21-hydroxyprogesterone; 1-OHP, 1-hydroxypyrene; LC-MS, liquid chromatography – mass spectrometry; LTG, lamotrigine; MOR, morphine; MPA, mycophenolic acid; 4-MU, 4-methylumbelliferone; 1-NAP, 1-naphthol; 4-NP, 4-nitrophenol; PE, phenethyl alcohol; S-NAP, S-naproxen; Sf9, clonal isolate from *Spodoptera frugiperda* IPLB-Sf21-AE cells; Sf9 membranes, membranes prepared from uninfected Sf9 cells; TFP, trifluoperazine; UDP-Glc, UDP-glucose; UDP-GlcUA, UDP-glucuronic acid; UGT, UDP-glucuronosyltransferase

ABSTRACT

Accumulating evidence indicates that several human UDP-glucuronosyltransferase enzymes catalyze both glucuronidation and glucosidation reactions. Baculovirus-infected insect cells (*Trichoplusia ni* and *Spodoptera frugiperda* (Sf9)) are used widely for the expression of recombinant human UGT enzymes. Following the observation that control Supersomes (c-SUP) express a native enzyme capable of glucosidating morphine, we characterized the glucosidation of a series of aglycones with either a hydroxyl (aliphatic or phenolic), carboxylic acid or amine functional group by c-SUP and membranes from uninfected Sf9 cells. Although both enzyme sources glucosidated the phenolic substrates investigated, albeit with differing activities, differences were observed in the selectivities of the native UDP-glucosyltransferases towards aliphatic alcohols, carboxylic acids, and amines. For example, zidovudine was solely glucosidated by c-SUP. By contrast, c-SUP lacked activity towards the amines lamotrigine and trifluoperazine and did not form the acyl glucoside of mycophenolic acid, reactions all catalyzed by uninfected Sf9 membranes. Glucosidation intrinsic clearances were high for several substrates, notably 1-hydroxypyrene (~1,400 – 1,900 $\mu\text{l}/\text{min}.\text{mg}$). The results underscore the importance of including control cell membranes in the investigation of drug and chemical glucosidation by UGT enzymes expressed in *T. ni* (High-Five™) and Sf9 cells. In a coincident study we observed that UGT1A5 expressed in Sf9, HEK293T and COS7 cells lacked glucuronidation activity towards prototypic phenolic substrates. However, Sf9 cells expressing UGT1A5 glucosidated 1-hydroxypyrene with UDP-glucuronic acid as the cofactor, presumably due to the presence of UDP-glucose as an impurity. Artefactual glucosidation may explain, at least in part, a previous report of phenolic glucuronidation by UGT1A5.

INTRODUCTION

Enzymes of the UDP-glucuronosyltransferase (UGT) family play a pivotal role in the clearance and detoxification of a structurally diverse range of substrates that include drugs, non-drug xenobiotics and endogenous compounds. The nineteen human UGT proteins classified in sub-families 1A, 2A and 2B primarily catalyze the transfer of glucuronic acid, from the cofactor UDP-glucuronic acid (UDP-GlcUA), to a typically lipophilic substrate (or aglycone) bearing a nucleophilic ‘acceptor’ functional group to form a glucuronide conjugate that is excreted in urine and/or bile (Mackenzie et al., 2005; Miners et al., 2010). By contrast, UGT 3A1 and 3A2 utilize UDP-sugars other than UDP-GlcUA (e.g. UDP-glucose (UDP-Glc), UDP-xylose and UDP-N-acetylglucosamine) as the cofactor (Mackenzie et al., 2008 and 2011). Although glucuronidation is the major metabolic pathway mediated by UGT 1A, 2A and 2B enzymes, 1A and 2B sub-family enzymes may additionally utilize sugar donors other than UDP-GlcUA, especially UDP-Glc. In particular, UGT2B7 catalyzes both the glucuronidation and glucosidation of a number of substrates, including morphine (MOR), forming phenolic-, acyl- and N- glucosides (Buchheit et al., 2011; Chau et al., 2014; Mackenzie et al., 2003; Tang et al., 2003; Toide et al., 2004). At least with MOR glycosidation by UGT2B7, glucuronidation predominates over glucosidation because the binding affinity of UDP-GlcUA is higher than that of UDP-Glc (Chau et al., 2014). Substrates of other UGT enzymes (e.g. 1A1, 1A9 and 2B10) have also been reported to form glycoside conjugates other than glucuronides (Feverly et al., 1977; Senafi et al., 1994; Lu et al., 2018; Chau and Miners, unpublished data). Despite the likelihood that UGT-catalyzed glucuronidation and glucosidation of xenobiotics may occur as complementary metabolic pathways, glucosidation has received little attention (Tang 1990; Meech et al., 2012).

It is well established that the individual human UGT enzymes exhibit distinct, but frequently overlapping, substrate and inhibitor selectivities (Miners et al., 2004 and 2010). In this regard, the availability of cDNA-expressed UGT proteins has been pivotal in the characterization of UGT function. Recombinant UGTs have been expressed in numerous mammalian and non-mammalian cell lines (Radomska-Pandya et al., 2005). Examples include COS (African Green Monkey kidney fibroblasts), HEK293T (Human Embryonic Kidney cell line), V79 (Chinese Hamster lung fibroblasts), yeast (*Pichia pastoris* and *Saccharomyces cerevisiae*), and baculovirus infected insect cells (*Spodoptera frugiperda* (Sf9) and *Trichoplusia ni*) (e.g. Fournel-Gigleux et al., 1991; Jin et al, 1997; Nguyen and Tukey, 1997; Ouzzine et al., 1999; Uchaipichat et al., 2004; Zhang et al., 2012). Of these, the use of commercially available UGT-expressing Supersomes™, prepared from baculovirus-infected *T. ni* cells, has become widespread in academia and industry. However, in a recent study of the comparative 3- glucuronidation and glucosidation of MOR by UGT2B7 we observed that Supersomes expressing UGT 2B4, 2B15 and 2B17 protein as well as control Supersomes (c-SUP; insect cell ‘control’ microsomes prepared from *T. ni* (High-Five™) cells infected with wild-type baculovirus) all exhibited significant and comparable MOR 3- glucosidation activities (Chau et al., 2014).

Since these data indicate that Supersomes express a ‘native’ enzyme capable of MOR 3- glucosidation, we characterized the glucosidation of a series of aglycones with either a phenolic (1-hydroxypyrene, 1-OHP; 4-methylumbelliferone, 4-MU; MOR; mycophenolic acid, MPA; 1-naphthol, 1-NAP; and 4-nitrophenol, 4-NP), aliphatic alcohol (codeine, COD; 21-hydroxyprogesterone, 21-OHPr; phenethyl alcohol, PE; and zidovudine, AZT), acyl (MPA; S-naproxen, S-NAP) or amine (benzocaine, BZC; lamotrigine, LTG; and trifluoperazine, TFP) acceptor functional group (see Supplemental Figure 1 for structures and

sites of conjugation) by c-SUP. The glucosidation of these aglycones was additionally characterized using the enriched membrane fraction from uninfected Sf9 cells (subsequently referred to as ‘Sf9 membranes’) since baculovirus-infected Sf9 cells are also used for UGT expression (e.g. Zhang et al., 2012) and are available commercially as Baculosomes™.

Coincident with these studies, we conducted an investigation of UGT1A5 structure-function. UGT1A5 expressed in baculovirus-infected Sf9 cells has been reported to glucuronidate a number of phenolic substrates, including 1-OHP and 4-MU (Finel et al., 2005). However, we found that UGT1A5 lacked glucuronidation activity when expressed in COS7, HEK293T and baculovirus-infected Sf9 cells. The glucosidation activity studies reported here indicate that 1-OHP, 4-MU and most other aglycones investigated are glucosidated by c-SUP and/or Sf9 cell membranes. It is possible that artefactual glucosidation by Sf9 membranes may contribute, at least in part, to the differing UGT1A5 glucuronidation data reported between laboratories.

MATERIALS AND METHODS

Materials

AZT, AZT β -D-glucuronide, codeine (COD), gentamicin, 21-OHPr, 1-OHP, kanamycin, 4-MU, 4-MU β -D-glucoside, 1-NAP, 1-NAP β -D-glucuronide, S-NAP, 4-NP, 1-octanesulfonic acid sodium salt, tetracycline, TFP, triethylamine, UDP-Glc (disodium salt) and UDP-GlcUA (trisodium salt) were purchased from Sigma-Aldrich (Sydney, NSW, Australia); BZC, COD β -D-glucuronide, 1-OHP β -D-glucuronide, MPA, MPA acyl β -D-glucoside, MPA phenolic β -D-glucoside, PE and PE β -D-glucoside, from Toronto Research Chemicals (Toronto, ON, Canada); 4-NP β -D-glucoside from Molekula Limited (Dorset, UK); BZC N-glucoside from Dalton Pharma Services (Toronto, ON, Canada); and MOR hydrochloride from GlaxoSmithKline (Melbourne, Vic, Australia). LTG and LTG N2-glucuronide were a gift from The Wellcome Foundation Ltd (London, UK). MOR 3- β -D-glucoside was synthesised in-house, as described by Chau et al. (2014). Microsomes from High-FiveTM cells infected with 'control' (wild-type) baculovirus (c-SUP) were purchased from Corning Gentest (BD Biosciences, North Ryde, NSW, Australia); uninfected Sf9 cells, penicillin-streptomycin solution (100 U/ml-100 μ g/ml), Cellfectin® reagent, and DH10BacTM *E. coli* cells from Invitrogen (Carlsbad, CA); COS7 and HEK293 cells from American Type Culture Collection (Manassas, VA); and Hyclone SFX-Insect Cell Culture medium and heat-inactivated Fetal Bovine Serum from ThermoFisher Scientific (Waltham, MA). Solvents and other reagents were of analytical reagent grade.

Methods

Glucosidation assay

Incubations, in a total volume of 200 μ l, contained phosphate buffer (0.1 M, pH 7.4 or pH 6.8 for carboxylic acid-containing substrates), MgCl_2 (4 mM), uninfected Sf9 cell membranes (1 mg/ml), substrate, and UDP-Glc (5 mM). After a 5 min pre-incubation at 37°C in a shaking water bath, reactions were initiated by the addition of UDP-Glc and performed for 2 hr. Reactions were terminated by the addition of either perchloric acid (70% v/v; 2 μ l), ascorbic acid in methanol (2% w/v; 200 μ l), or acetic acid in methanol (4% v/v; 200 μ l), depending on the substrate (Supplemental Table 1) and cooling on ice for 10 min. Samples were centrifuged (5000 g for 10 min), and a 5 - 40 μ l aliquot of the supernatant fraction was analyzed by HPLC. Rates of glucoside formation were measured at four different substrate concentrations (see *Results*). Experiments utilizing c-SUP as the enzyme source were as described for Sf9 membranes, except the incubation volume was 100 μ l. Incubations were performed at least in duplicate (<5% variance between replicates). Incubations for MS analysis followed the above protocols, except reactions were terminated by the addition of two volumes of MS-grade 4% acetic acid in methanol or 2% ascorbic acid in methanol (BZC glucosidation assay).

Incubation conditions for studies characterizing glucosidation kinetic parameters for 1-OHP, MPA (phenolic and acyl), MOR and 4-MU with both c-SUP and uninfected Sf9 membranes as the enzyme source were as described above, with the following changes to protein concentrations and incubation times: 1-OHP (0.01 mg/ml, 15 min), MOR (1 mg/ml, 60 min), MPA (0.1 mg/ml, 15 min) and 4-MU (0.1 mg/ml, 30 min). Kinetic studies included 11 or 12 substrate concentrations that spanned the K_m (or S_{50}).

Quantification of glucoside conjugate formation by HPLC

Glucoside conjugates were measured by reversed-phase HPLC using an Agilent 1100 series instrument (Agilent Technologies, Sydney, Australia) comprising an auto-injector, a

quaternary solvent delivery system and a UV detector (1200 series). Analytes were separated using varying chromatographic conditions, depending on the aglycone. Columns, mobile phases, absorbance wavelengths, precipitating agent, retention times of glucosides, detection method and wavelength, and injection volume are given in Supplemental Table 1. Glucoside formation was quantified by comparison of peak areas to those of a standard curve; authentic glucoside conjugates were available for BZC, 21-OHPr, MPA, MOR, 4-MU and 4-NP. Where the glucoside was unavailable, either the corresponding glucuronide (AZT, COD, LTG, 1-NAP and 1-OHP) or aglycone (S-NAP and TFP) were used for standard curve generation. The identity of the glucoside conjugates was confirmed by co-chromatography with the authentic standard (where available) and from the m/z ratios and fragmentation patterns generated by LC-MS (see below). Calibration curves included 5 concentrations, the ranges of which are given in Supplemental Table 1.

Confirmation of glucoside formation by UPLC-MS

Glucoside conjugates were separated and detected using a Waters ACQUITY™ Ultra Performance Liquid Chromatography (UPLC) system coupled to a Waters Micromass Q-TOF Premier™ mass spectrometer (Waters Corporation Micromass UK Ltd., Manchester, UK). Analytes were separated on an ACQUITY UPLC® HSST3 column (1.8 µm particle size, 2.1×100 mm; Waters Corporation, Milford, MA, USA). The mobile phase, delivered at a flow rate of 0.25 ml/min, consisted of two solutions (phase A, 100% MS-grade acetonitrile; phase B, 5% acetonitrile in water) mixed according to a gradient timetable. Initial conditions were 5% phase A - 95% phase B held for 3 min followed by a linear gradient over 7 min to 60% phase A - 40% phase B, which was held constant for 0.5 min. The total run time, including reconditioning of the column to initial conditions, was 12.5 min. The MS operated in positive ion mode with electrospray ionization (ESI+). Time-of-flight data (ToF) data were

acquired in selected ion (MS^E) mode, where the first resolving quadrupole acquired mass data from m/z 100 to 1000. Collision cell energy alternated between 2 eV and a high energy ramp (3 to 15 eV). The cone and desolvation gases were set to flow rates of 50 and 550 l/hr, respectively; desolvation and source temperatures were 250°C and 90°C, respectively; and capillary and cone voltages were 1,800 and 25 V, respectively. MS data were collected as total ion chromatograms, with selected ion (pseudo MRM) data extracted at the $[M + H^+]$ for each analyte of interest using Waters QuanLynxTM software (Waters Corporation).

Construction of recombinant baculovirus

The preparation of the human UGT1A5 cDNA (NM_019078) from epithelial colorectal adenocarcinoma (Caco-2) cells has been described previously by Finel et al. (2005). For expression in Sf9 cells, the cDNA was subcloned into the pFastBac-HT vector (Invitrogen, Carlsbad, CA, USA) using XhoI and HindIII restriction sites and the engineered pFB-UGT1A5-His sequence confirmed on both strands (ABI 3130-XL DNA sequencer; Applied Biosystems, Vic, Australia). Generation of recombinant Bacmid DNA was achieved by transposition of the UGT1A5 cDNA from pFastBac-HT (1 ng) to the viral genome of DH10Bac chemically competent *E. coli* cells (50 μ l). Recombinant Bacmid DNA was amplified (100 ml culture) and purified (Plasmid Midi Kit; Qiagen, Hilden, Germany). PCR analysis of the recombinant Bacmid DNA was performed to identify the presence of UGT1A5 in the AcMNPV viral genome using the pUC/M13 forward and reverse primers.

Expression of UGT1A5 in Sf9 cells and separation of Sf9 membranes

Sf9 cells adapted to suspension culture were grown in SFX-Insect medium supplemented with heat inactivated FBS (5%) and penicillin-streptomycin (1000 U and 1 mg). Cells were seeded (5×10^5 cell/ml) and cultured in glass impeller spinner flasks (Bellco Glass, Inc.,

Vineland, NJ, USA) at 28°C and 120 rpm (50% spinner volume) in exponential growth phase with a cell density between 1×10^6 to 2.5×10^6 cells/ml at greater than 95% viability. Infection optimization for UGT1A5 expression was undertaken in monolayer cultures of Sf9 cells using the Cellfectin method described by the manufacturer (Invitrogen, Carlsbad, CA, USA). Large-scale expression of UGT1A5 was performed in 1 l shaker flasks with Sf9 cells in mid-logarithmic growth at a seeding density of 1×10^6 cell/ml. Cells were infected with AcMNPV-UGT1A5 at multiplicity of infection 10 (150 μ L; 2×10^8 pfu/ml) and harvested 48 h post-infection by centrifugation at 850 g for 10 min.

The enriched membrane fraction from both Sf9 cells infected with UGT1A5-containing Bacmid (i.e. expressing UGT1A5) and uninfected Sf9 cells was isolated by sonication and ultracentrifugation. Pelleted cells were resuspended in cold deionized water (0.33 g pellet/ml), homogenized with 15 strokes using a Potter Elvehjem homogenizer, sonicated by eight 1 sec ‘bursts’, each separated by 1 min cooling on ice, using a Vibra Cell VCX 130 Ultrasonics Processor (Sonics and Materials, Newton, CT), and then centrifuged at 10,000 g for 10 min at 4°C. The supernatant fraction was decanted and centrifuged at 105,000 g at 4°C for 75 min. The pellet, which comprised the enriched membrane fraction, was resuspended in phosphate buffer (0.1 M, pH 7.4) and stored at -80°C until use.

The UGT1A5 cDNA, cloned in the pEF-IRES-puro 6 vector, was stably expressed in HEK293T and COS7 cells using the procedure described by Uchaipichat et al. (2004), and cell lysates were employed for immunoblotting and assessment of enzyme activity.

Immunoblotting

Cell lysates from transfected HEK293T and COS7 cells and Sf9 membranes expressing UGT1A5 protein (20-100 μ g) were separated by 10% SDS-polyacrylamide gel

electrophoresis and rectilinearly transferred to nitrocellulose (0.45 μ m; Bio-Rad laboratories, Hercules, CA, USA). Immunodetection of UGT1A5 protein was performed using the WB-Human UGT1A Western Blotting Kit (BD Gentest, Woburn, MA, USA). Nitrocellulose membranes were incubated with rabbit anti-UGT1A subfamily IgG as the primary antibody (1:1500 dilution) followed by HRP-conjugated goat anti-rabbit IgG (Thermo Scientific, Rockland, IL) as the secondary antibody (1:2000 dilution). Additionally, Sf9 expressed UGT1A5 was probed with His-tag recognizing primary polyclonal antisera (rabbit anti-human His-tagged UGT2B7) developed in this laboratory (Kerdpin et al. 2009). This antibody was raised to residues 55 to 165 of UGT2B7 and expressed in *E. coli* with a C-terminus 6-histidine tag at the C-terminus, and hence recognizes His-tagged proteins. The primary antisera (1:1500 dilution) was detected using HRP-conjugated goat anti-rabbit IgG (1:2000 dilution). Immunoreactivity was detected by chemiluminescence (Roche Diagnostics GmbH, Mannheim, Germany). Blots were visualised with a Fujifilm LAS-4000 imaging system (Fujifilm Life Sciences, NSW, Australia) and band intensities measured using Multi Gauge software (Fujifilm Life Sciences, NSW, Australia). Relative UGT1A5 protein levels represent the mean of triplicate measurements. Western blot analysis and activity assays were performed using the same batch of cell lysate.

Data analysis

Activity and kinetic data from experiments using uninfected Sf9 membranes and c-SUP represent the mean of duplicate measurements, unless otherwise indicated. For generation of kinetic constants, the Michaelis-Menten, Hill and substrate inhibition equations (see below) were fit to untransformed experimental data using Enzfitter (Biosoft, Cambridge, UK) to generate kinetic parameters. Goodness of fit was assessed from the coefficient of determination (r^2), F-statistic, 95% confidence intervals and standard error of the fit.

Duplicate data were pooled for model-fitting. Kinetic data are shown as Eadie-Hofstee plots (velocity versus velocity/ [substrate]) and kinetic constants are reported as the parameter \pm standard error of the parameter fit.

Michaelis-Menten equation

$$v = \frac{V_{\max} \times [S]}{K_m + [S]}$$

where v is the rate of metabolite formation, V_{\max} is the maximum velocity (as pmol/min.mg microsomal or cell lysate protein, $[S]$ is the substrate concentration, K_m is the Michaelis constant (substrate concentration at 0.5 V_{\max}).

Hill equation

$$v = \frac{V_{\max} \times [S]^n}{S_{50} + [S]^n}$$

where S_{50} is the Hill constant (substrate concentration at 0.5 V_{\max}) and n is the Hill coefficient ($n < 1$ = negative cooperativity and $n > 1$ = positive cooperativity).

Substrate inhibition

$$v = \frac{V_{\max}}{1 + \frac{K_m}{[S]} + \frac{[S]}{K_{si}}}$$

where K_{si} is the substrate inhibition constant.

Intrinsic clearance (Cl_{int}) was calculated as V_{\max}/K_m .

RESULTS

Opioid glucosidation

We have reported previously that both c-SUP and Supersomes expressing UGT2B7 catalyze the 3-glucosidation, but not the 6-glucosidation, of MOR in the presence of UDP-Glc as co-factor (Chau et al., 2014). Thus, the kinetics of MOR 3-glucosidation by c-SUP and Sf9 membranes, were characterized using 11 substrate concentrations from 0.05 to 10 mM. Kinetic parameters are given as the mean of duplicate measurements \pm SE of the parameter fit. MOR 3-glucosidation by c-SUP exhibited hyperbolic (Michaelis-Menten) kinetics, whereas negative cooperative kinetics ($n = 0.96 \pm 0.01$) was observed with Sf9 membranes (Figure 1). Respective mean K_m (or S_{50}) and V_{max} values for MOR 3-glucosidation by c-SUP and Sf9 membranes were 3.4 ± 0.001 and 4.4 ± 0.07 mM, and 266 ± 9.3 and 362 ± 2.5 pmol/min.mg. In contrast to MOR, which has both phenolic (3-position) and enolic (6-position) hydroxyl groups, COD has only an enolic hydroxyl group at the 6-position. Consistent with the lack of MOR 6-glucosidation by c-SUP and Sf9 membranes, COD was not glucosidated by these enzyme sources.

Activity of uninfected Sf9 membranes and c-SUP towards hydroxyl-, carboxylic acid- and amine- containing aglycones

Screening studies were performed to further characterize the glucosidation capacity and selectivity of Sf9 membranes and c-SUP. Twelve substrates that contained either an aliphatic or phenolic hydroxyl, or carboxylic acid or amine functional group were investigated. The activity profile of each substrate was determined at four concentrations that provided a meaningful activity range while maintaining aglycone solubility in the incubation medium.

Glucosidation of substrates containing a hydroxyl group: In addition to MOR and COD, a further eight compounds containing a phenolic or aliphatic hydroxyl group were screened for glucosidation by c-SUP and Sf9 membranes with UDP-Glc as cofactor (Figure 2); 21-OHPr, 1-OHP, 4-MU, MPA, 1-NAP, 4-NP, PE and AZT. AZT was glucosidated only by c-SUP (Figure 2H). The rates of glucosidation of 21-OHPr, 1-OHP and 1-NAP were higher with cSUP compared to Sf9 membranes (Figures 2A, 2B and 2E). At the highest aglycone concentration investigated, rates of glucosidation were approximately 22-, 28- and 2.7- fold higher for 21-OHPr, 1-OHP and 1-NAP, respectively. By contrast, the rates of formation of the glucosides of PE and MPA (phenolic) by Sf9 membranes were approximately 4- to 10.5- and 3- to 6- fold and higher, respectively, compared to c-SUP (Figures 2D and 2H). The rates of 4-MU and 4-NP glucosidation were reasonably similar with both enzyme sources (Figures 2C and 2F)

To further characterize the glucosidation of hydroxyl-containing substrates, the kinetics of 1-OHP (Figure 3A and B), MPA (Figure 3C and D) and 4-MU (Figure 3E and F) glucosidation by c-SUP and Sf9 membranes was investigated using 11 or 12 aglycone concentrations that spanned the K_m (or S_{50}). Substrate concentration ranges are given in the legend to Figure 3. Best fit kinetic equations were consistent with the activity data shown in Figure 2 and, as observed with MOR, the equation of best fit differed between the two enzyme sources for 1-OHP and MPA. 1-OHP glucosidation by c-SUP exhibited negative cooperative kinetics ($n = 0.89 \pm 0.01$), but weak substrate inhibition ($K_{si} = 13.3 \pm 1.9 \mu M$) with Sf9 membranes. Respective mean K_m or S_{50} and V_{max} values for 1-OHP glucosidation by c-SUP and Sf9 membranes were 8.0 ± 0.21 and $1.4 \pm 0.11 \mu M$ and $11,211 \pm 144$ and $2,713 \pm 132$ pmol/min.mg, respectively. MPA phenolic glucosidation by c-SUP and Sf9 membranes were best described by the Michaelis-Menten and substrate inhibition equations, respectively;

mean and V_{\max} values for MPA phenolic glucosidation by c-SUP and Sf9 membranes were 165 ± 0.35 and 15.5 ± 1.1 μM ($K_{\text{si}} = 2998 \pm 468$ μM), and 916 ± 0.81 and $4,076 \pm 97$ pmol/min.mg, respectively. 4-MU glucosidation by both c-SUP and Sf9 membranes exhibited negative cooperative kinetics with mean n , S_{50} and V_{\max} values of 0.85 ± 0.003 , 282 ± 2.6 μM and $2,390 \pm 9.3$ pmol/min.mg, and 0.91 ± 0.03 , 123 ± 8.3 μM and $2,580 \pm 63$ pmol/min.mg, respectively.

Glucosidation of carboxylic acid- and amine-containing substrates: Rates of the acyl glucosidation of MPA and S-NAP, and the N-glucosidation of the amines BZC, LTG and TFP by c-SUP and Sf9 membranes are shown in Figure 2. Rates of S-NAP glucosidation were substantially higher (3- to 16- fold) with Sf9 membranes than with c-SUP (Figure 2J). MPA acyl glucosidation was observed only with Sf9 membranes at the highest aglycone concentration (Figure 2I). Similarly, LTG and TFP were glucosidated solely by Sf9 membranes (Figures 2L and 2M), and rates of BZC N-glucosidation by Sf9 membranes more than double those of c-SUP (Figure 2K).

Verification of glucoside formation by c-SUP and uninfected Sf9 membranes

Peaks corresponding to glucoside conjugates were not observed in chromatograms from experiments performed in the absence of UDP-Glc. As noted in *Methods*, authentic glucoside conjugates were available for BZC, 21-OHPr, MPA, 4-MU and 4-NP. Glucosidation of these compounds was confirmed by comparison of HPLC retention times with those of authentic standards. In addition, the formation of a glucoside conjugate of the substrates investigated here was confirmed by LC-MS. Observed and predicted m/z values for glucosides, except that of 4-NP, are shown in Table 1. In addition, fragmentation patterns were consistent with glucoside formation (data not shown). An m/z value corresponding to 4-NP glucoside could not be detected by MS in positive ion mode, even for the authentic standard, despite detection

by HPLC and UPLC. However, the fragmentation pattern was consistent with formation of 4-NP glucoside.

Expression and activity of UGT1A5 in mammalian (HEK293T and COS7) and insect (Sf9) cell lines

Initial experiments sought to express human UGT1A5 in HEK293T and COS7 cells.

Expression of UGT1A5 protein was not apparent in HEK293T cells (Figure 4A), but weak expression was observed in COS7 cell lysate (Figure 4B). Although 1-OHP has been reported to be glucuronidated by UGT1A5 (Finel et al, 2005), glucuronidation of this substrate was not observed with either the transfected HEK293T or COS7 cell lysates. 1-OHP glucuronidation was confirmed with human liver microsomes as the positive control (data not shown).

Given the lack of or weak expression of UGT1A5 in the mammalian cell lines and the lack of observed 1-OHP glucuronidation activity, baculovirus-mediated expression of His-tagged UGT1A5 in Sf9 cells was undertaken. Western blot analysis using an antibody that recognizes His-tagged proteins identified a band with the expected molecular mass of UGT1A5 (Figure 4C). As with the mammalian expression systems, the UGT1A5 protein expressed in Sf9 cells lacked glucuronidation activity towards 1-OHP. However, incubations of the enriched membrane fraction of Sf9 cells expressing UGT1A5 and uninfected Sf9 cells with UDP-GlcUA as the added cofactor showed the presence of a peak that chromatographed with almost the same retention time as 1-OHP glucuronide. The second peak was identified as 1-OHP glucoside by LC-MS and by comparison of the HPLC retention time with that of the authentic standard. Incubation of uninfected Sf9 cell membranes supplemented with UDP-Glc as cofactor resulted in the formation of a 1-OHP glucoside peak that had an approximate 800-fold greater area than the peak formed with UDP-GlcUA as cofactor. The 1-OHP glucoside peak that formed with UDP-GlcUA as cofactor was presumed to arise from

the presence of UDP-Glc as an impurity in commercial UDP-GlcUA. HEK293T, COS7 and Sf9 cells engineered to express recombinant UGT1A5 were additionally screened for 1-NAP, 4-MU, TFP and LTG glucuronidation, but no activity was observed. UGT1A6 and UGT1A4 expressed in HEK293T cells were used as positive controls for the glucuronidation of 4-MU/1-NAP and TFP/LTG, respectively, as described by Uchaipichat et al. (2006) and Kubota et al. (2007).

DISCUSSION

There is increasing evidence demonstrating that several human UGT 1A and 2B subfamily enzymes may catalyze both glucuronidation and glucosidation reactions. Indeed, the importance of glucosidation as a drug and chemical biotransformation pathway may be underestimated (see Introduction). Recombinant UGT enzymes are used extensively for the reaction phenotyping of drug glucuronidation (Miners et al, 2010; Zientek and Youdim, 2015), and have also been utilized to investigate glucosidation (e.g. Buchheit et al, 2011; Chau et al, 2014; Mackenzie et al, 2003; Tang et al, 2003; Toide et al, 2004). Numerous mammalian and non-mammalian expression systems are employed for the generation of recombinant UGT proteins, including baculovirus-infected insect (Sf9 and *T. ni*) cells (Radomska-Pandya et al, 2005). Recombinant human UGT enzymes expressed in insect cells are available commercially (e.g. Baculosomes, Supersomes) and are used widely by both Academic and Industry laboratories. We reported recently that c-SUP efficiently catalyzed the glucosidation (with UDPGlc as cofactor), but not glucuronidation, of MOR suggesting that insect cells used for the generation of recombinant UGTs may express an endogenous UDP-glycosyltransferase(s) capable of glucosidating drugs and other chemicals. This prompted us to investigate the glucosidation of a series of aglycones with either a phenolic (1-OHP, 4-MU, MOR, MPA, 1-NAP and 4-NP), aliphatic alcohol (COD, 21-OHPr, PE and AZT), acyl (MPA and S-NAP) or amine (BZC, LTG and TFP) acceptor functional group (see Supplemental Figure 1 for structures) by c-SUP and Sf9 membranes in order to characterize the scope and selectivity of drug and chemical glucosidation by these insect cell lines. All of the compounds investigated are known to be glucuronidated by human liver microsomes and/or recombinant UGTs (Green and Tephly 1996; Shipkova et al., 2001; Stone et al., 2003; Uchaipichat et al. 2004 and 2006; Finel et al. 2005; Rowland et al. 2006; Bowalgaha et al. 2007; Gaganis et al., 2007; Kubota et al., 2007; Raungrut et al, 2010).

Differences were observed in the substrate selectivities and activities of the native UDP-glucosyltransferases of c-SUP and Sf9 membranes. Amongst the phenols, rates of 1-OHP and 1-NAP glucosidation were substantially higher with c-SUP, while MPA was preferentially glucosidated by Sf9 membranes. Rates of glucosidation of 4-MU and 4-NP were similar with both enzyme sources. The aliphatic alcohols AZT and 21-OHPr were solely or preferentially glucosidated by c-SUP, while rates of PE glucosidation were higher with Sf9 membranes. Neither c-SUP nor Sf9 membranes glucosidated MOR and COD at the 6- (enolic) position. Sf9 membranes glucosidated the carboxylic acid functional group of MPA and S-NAP, and N-glucosidated BZC, LTG and TFP. By contrast, glucosidation activity of c-SUP was not measurable (MPA, LTG and TFP) or low in comparison to Sf9 membranes (S-NAP and BZC).

Differences in the kinetics of 1-OHP, MPA and MOR (3-position) glucosidation were also observed between the two enzyme sources: 1-OHP, negative cooperative (c-SUP) and substrate inhibition (Sf9); MPA, Michaelis-Menten (c-SUP) and substrate inhibition (Sf9); and MOR, Michaelis-Menten (c-SUP) and substrate inhibition (Sf9). By contrast, 4-MU glucosidation by both enzyme sources exhibited negative cooperative kinetics. When data are considered as intrinsic clearances (calculated as K_m or S_{50} divided by V_{max} , noting that n values were close to 1 for substrates exhibiting negative cooperative kinetics), ratios (c-SUP/Sf9 membranes) were of a similar order for 1-OHP (0.73), MOR (0.95) and 4-MU (0.40), but considerably lower for MPA (0.02). By way of comparison, the K_m/S_{50} values for MOR 3-glucosidation by c-SUP and Sf9 membranes (3.42 – 4.40 mM) were similar to the K_m (5.56 mM) reported for MOR 3-glucosidation by human liver microsomes, although the V_{max} was lower (Chau et al, 2014). Notably, 1-OHP was glucosidated very efficiently c-SUP and Sf9 membranes, with respective Cl_{int} values of 1,409 and 1,938 $\mu\text{l}/\text{min}.\text{mg}$.

Taken together, the results demonstrate that c-SUP and Sf9 membranes have the capacity to glucosidate both drugs and non-drug xenobiotics. However, differences occur between the native UDP-glucosyltransferases of c-SUP and Sf9 membranes. Although neither c-SUP nor Sf9 membranes catalyzed the 6-glucosidation of COD and MOR and Cl_{int} ratios were similar for several phenols (1-OHP, MOR and 4-MU), Sf9 membranes preferentially glucosidated MPA while the aliphatic alcohols 21-OHPr and AZT were glucosidated almost exclusively by c-SUP. Sf9 membranes exclusively or preferentially glucosidated the carboxylic acid- and amine- containing aglycones investigated here.

While it is acknowledged that too few compounds were studied to establish meaningful structure-function relationships, it is apparent that care is required when investigating drug and chemical glucosidation by recombinant UGT enzymes expressed in insect cells. As noted previously, there is evidence demonstrating that UGT-catalyzed glucuronidation and glucosidation may occur as complementary metabolic pathways for xenobiotics. For example, we observed MOR 3-glucosidation by Supersomes expressing UGT2B4, UGT2B7, UGT2B15 and UGT2B17, but activity was only apparent for UGT2B7 when the background activity of c-SUP was taken into account (Chau et al, 2014). By contrast, HEK293 cells do not express an endogenous UDP-glycosyltransferase capable of glucosidating MOR and other xenobiotics (Chau et al, 2014). The data emphasize the requirement for ‘control’ cell lysate/membranes in the investigation of drug and chemical glucosidation (and possibly conjugation with other sugars) by recombinant enzymes expressed in insect cells. It is known that many insect species, including lepidopterans (which include *S. frugiperda* and *T. ni*), express UDP-glycosyltransferases that preferentially utilize UDP-Glc as cofactor for the metabolism of dietary and environmental chemicals (Meech et al, 2012; Ahn et al, 2012). It has also been proposed that insect viruses have evolved UDP-glycosyltransferases that

apparently facilitate exploitation of insect larvae as hosts for reproduction (Meech et al, 2012), although it is unknown whether the viral vector (AcMNPV) used here expresses a xenobiotic UDP-glucosyltransferase.

Coincident with the study investigating xenobiotic glucosidation by c-SUP and uninfected Sf9 membranes, we commenced an investigation of UGT1A5 structure-function. UGT1A5 expressed in Sf9 cells has been reported to readily glucuronidate 1-OHP (Finel et al, 2005). Using UDP-GlcUA as cofactor, the rate of 1-OHP glucuronidation (at a substrate concentration of 500 μ M) by UGT1A5 was 97 pmol/min.mg. By contrast, rates of glucuronidation of 4-MU and scopoletin were low, approximately 1 pmol/min.mg. In the present work, weak expression of UGT1A5 was observed in COS7 cells, but expression was not apparent in HEK293T cells using a commercial UGT1A subfamily antibody. Moreover, 1-OHP glucuronidation was not observed with lysates of COS7 and HEK293T cells, despite being readily measurable with human liver microsomes as the enzyme source (approximately 5,000 pmol/min.mg at a substrate concentration of 40 μ M). Thus, we expressed His-tagged UGT1A5 in Sf9 cells as described by Finel and colleagues, including use of the same cDNA. Despite demonstration of His-tagged UGT1A5 protein expression by immunoblotting, the enzyme did not glucuronidate 1-OHP and 4-MU. No product was observed that co-chromatographed with authentic 1-OHP glucuronide or 4-MU glucuronide, nor was a peak with the expected m/z ratio and fragmentation pattern for 1-OHP glucuronide observed using LC-MS. However, formation of 1-OHP glucoside was verified by HPLC and LC-MS. It was presumed that glucoside formation occurred due to the presence of UDP-Glc as an impurity in UDP-GlcUA, but this was not confirmed at the time. The stated purity of the UDP-GlcUA (trisodium salt) used in experiments is 98 – 100%. There is anecdotal evidence suggesting that, at least in the past, UDP-Glc was present as an impurity in the trisodium salt of UDP-

GlcUA (but probably not in the tri-ammonium salt). Use of UDP-Glc as cofactor with UGT1A5 expressed in Sf9 cells gave a 1-OHP glucoside peak with a peak area approximately 800-fold higher than that observed with incubations conducted in the presence of UDP-GlcUA. In addition to wild-type UGT1A5, the Thr36Ile and His40Pro mutants were generated here. The mutants expressed in all three cell lines, albeit weakly in COS7 cells (Figure 4). Like wild-type UGT1A5, however, the mutants did not glucuronidate 1-OHP and 4-MU, nor the prototypic UGT1A4 substrates LTG and TFP (data not shown).

While artefactual glucosidation of 4-MU (and possibly scopoletin) may account for differences in the data presented here and by Finel et al. (2005), the relatively high rate of 1-OHP glucuronidation by UGT1A5 reported previously would seem inconsistent with glucosidation arising from the presence of UDP-Glc as an impurity in UDP-GlcUA. Nevertheless, identification of the glycoside conjugates(s) formed by incubations of insect cell membranes with UDP-GlcUA is recommended, especially when the rate of product formation is low. In addition to Finel et al. (2005) and the work presented here, UGT1A5 expressed in COS7 cells has been reported to glucuronidate 7-ethyl-10-hydroxy-camptothecin (SN-38), but the rate of glucuronidation was extremely low (ca. 100 pmol/16hr.mg, equivalent to 0.1 pmol/min.mg) and a non-specific radiometric TLC method was used for product quantification (Ciotti et al, 1999). More recently, Yang et al. (2018) described the expression of active UGT1A5 and two polymorphic variants (UGT1A5*8 and UGT1A5*9) in fission yeast (*Schizosaccharomyces pombe*) cells. The activities of Triton X-100 permeabilized cells expressing the UGT1A5 enzymes were investigated using the UGT-Glo assay (Promega), which measures the depletion of pro-luciferin substrates (UGT-Glo substrates A and B) rather than metabolite formation. Moreover, the activity (or lack thereof)

of control (untransformed) fission yeast cells was not reported. Further studies are required to unambiguously characterize the functional role of UGT1A5.

ACKNOWLEDGEMENT

Technical support from Mr David Elliot is acknowledged. The authors are grateful to Dr Andrew Rowland for his helpful advice.

AUTHORSHIP CONTRIBUTIONS

Participated in research design: Miners, Chau, Lewis and Mackenzie

Conducted experiments: Chau and Kaya

Performed data analysis: Miners, Chau and Lewis

Wrote or contributed to the writing of the paper: Miners, Chau, Mackenzie and Lewis

REFERENCES

- Ahn SJ, Vogel H, and Heckel DG (2012) Comparative analysis of the UDP-glycosyltransferase multigene family in insects', *Insect Biochem Mol Biol* **42**:133-147.
- Bowalgaha K, Elliot DJ, Mackenzie PI, Knights KM, and Miners, JO (2007) The glucuronidation of Delta(4)-3-keto C19- and C21-hydroxysteroids by human liver microsomal and recombinant UDP-glucuronosyltransferases (UGTs): 6 alpha- and 21-hydroxyprogesterone are selective substrates for UGT2B7. *Drug Metab Dispos* **35**: 363-370.
- Buchheit D, Dragan CA, Schmitt EI, and Bureik M (2011) Production of ibuprofen acyl glucosides by human UGT2B7. *Drug Metab Dispos*, **39**:2174-2181.
- Chau N, Elliot, DJ Lewis BC, Burns K, Johnston MR, Mackenzie PI, and Miners JO (2014) Morphine glucuronidation and glucosidation represent complementary metabolic pathways that are both catalyzed by UDP-glucuronosyltransferase 2B7: kinetic, inhibition, and molecular modeling studies. *J Pharmacol Exp Ther* **349**:126-137.
- Ciotti M, Basu N, Brangi M, and Owens IS (1999) Glucuronidation of 7-ethyl-10-hydroxycamptothecin (SN-38) by the human UDP-glucuronosyltransferases encoded at the UGT1 locus. *Biochem Biophys Res Commun* **260**:199-202.
- Feverly J, van de Vijver M, Michiels R, and Heirwegh KPM (1977) Comparison in different species of biliary bilirubin-IX α conjugates with the activities of hepatic and renal bilirubin-IX α -uridine diphosphate glycosyltransferases. *Biochem J* **164**:737-746.
- Finel M, Li X, Gardner-Stephen D, Bratton S, Mackenzie PI, and Radomska-Pandya A (2005) Human UDP-Glucuronosyltransferase 1A5: Identification, expression, and activity. *J Pharmacol Exp Ther* **315**:1143-1149.

Fournel-Gigleux S, Sutherland L, Sabolovic N, Burchell B, and Siest G (1991) Stable expression of two human UDP-glucuronosyltransferase cDNAs in V79 cultures. *Molec Pharmacol* **39**:177-183.

Gaganis P, Miners JO, Brennan JS, Thomas A, Knights KM (2007) Human renal cortical and medullary UDP-glucuronosyltransferases (UGTs): immunohistochemical localization of UGT2B7 and UGT1A enzymes and kinetic characterization of S-naproxen glucuronidation, *J Pharmacol Exp Ther* **323**:422-430.

Green MD and Tephly (1996) Glucuronidation of amines and hydroxylated xenobiotics and endobiotics catalyzed by expressed human UGT1.4 protein. *Drug Metab Dispos* **24**:356-363.

Jin C-J, Mackenzie PI, and Miners JO (1997) Regio- and stereo-selectivity of C19- and C21-hydroxysteroid glucuronidation by UGT2B7 and UGT2B11. *Arch Biochem Biophys* **341**: 207-212.

Kerdpin O, Mackenzie PI, Bowalgaha K, Finel M, and Miners, JO (2009) Influence of N-terminal domain histidine and proline residues on the substrate selectivities of human UDP-glucuronosyltransferase 1A1, 1A6, 1A9, 2B7, and 2B10. *Drug Metab Dispos* **37**:1948-1955.

Kubota T, Lewis BC, Elliot DJ, Mackenzie PI, and Miners JO (2007) Critical roles of residues 36 and 40 in the phenol and tertiary amine aglycone substrate selectivities of UDP-glucuronosyltransferases 1A3 and 1A4. *Molec Pharmacol* **72**:1054-1062.

Lu D, Dong D, Xie Q, Li Z, and Wu W (2018) Disposition of mianserin and cyclizine in UGT2B10-overexpressing HEK293 cells: Identification of UGT2B10 as a novel N-glucosidation enzyme and BCRP as an N-glucoside transporter. *Drug Metab Dispos* (doi.org/10.1124/dmd.118.080804)

Mackenzie P, Little JM, and Radomska-Pandya A (2003) Glucosidation of hyodeoxycholic acid by UDP-glucuronosyltransferase 2B7. *Biochem Pharmacol* **65**:417-421.

Mackenzie PI, Bock KW, Burchell B, Guillemette C, Ikushiro S, Iyanagi T, Miners JO, Owens IS, and Nebert DW (2005) Nomenclature update for the mammalian UDP glycosyltransferase (UGT) gene superfamily. *Pharmacogenet Genomics* **15**:677-685.

Mackenzie PI, Rogers A, Elliot DJ, Chau N, Hulin JA, Miners JO, and Meech R (2011) The novel UDP glycosyltransferase 3A2: Cloning, catalytic properties, and tissue distribution. *Molec Pharmacol* **79**:472-478.

Mackenzie PI, Rogers A, Treloar J, Jorgensen BR, Miners JO, and Meech R (2008) Identification of UDP glycosyltransferase 3A1 as a UDP N- acetylglucosaminyltransferase. *J Biol Chem* **283**:36205-36210.

Meech R, Miners JO, Lewis BC, and Mackenzie PI (2012) The glycosidation of xenobiotics and endogenous compounds: Versatility and redundancy in the UDP glycosyltransferase superfamily. *Pharmacol Ther* **134**:200-218.

Miners JO, Smith PA, Sorich MJ, McKinnon RA, and Mackenzie PI (2004) Predicting human drug glucuronidation parameters: Application of in vitro and in silico modeling approaches. *Ann Rev Pharmacol Toxicol* **44**:1-25.

Miners JO, Mackenzie PI and Knights KM (2010) The prediction of drug glucuronidation parameters in humans: UDP-glucuronosyltransferase enzyme selective substrate and inhibitor probes for reaction phenotyping and in vitro – in vivo extrapolation of drug clearance and drug-drug interaction potential. *Drug Metab Rev* **42**:196-208.

Ouzzine M, Magdalou J, Burchell B, and Fournel-Gigleux S (1999) An internal signal sequence mediates the targeting and retention of UDP-glucuronosyltransferase 1A6 to the endoplasmic reticulum. *J Biol Chem* **274**:31401-31409.

- Nguyen N and Tukey RH (1997) Baculovirus-directed expression of rabbit UDP-glucuronosyltransferases in *Spodoptera frugiperda* cells. *Drug Metab Dispos* **25**:745-749.
- Radomska-Pandya A, Bratton S, and Little JM (2005) A historical overview of the heterologous expression of mammalian UDP-glucuronosyltransferase isoforms over the past twenty years. *Curr Drug Metab* **6**:141-160.
- Raungrut P, Uchaipichat V, Elliot DJ, Janchawee B, Somogyi AA, and Miners JO (2010) In vitro – in vivo extrapolation predicts drug-interactions arising from inhibition of codeine glucuronidation by dextropropoxyphene, fluconazole, ketoconazole and methadone in humans. *J Pharmacol Exp Ther* **334**: 609-618.
- Rowland A, Elliot DJ, Williams JA, MacKenzie PI, Dickinson RG, and Miners JO (2006) In vitro characterization of lamotrigine N2-glucuronidation and the lamotrigine-valproic acid interaction. *Drug Metab Dispos* **34**:1055-1062.
- Senafi SB, Clarke DJ, and Burchell B (1994) Investigation of the substrate-specificity of a cloned expressed human bilirubin UDP-glucuronosyltransferase - UDP-sugar specificity and involvement in steroid and xenobiotic glucuronidation. *Biochem J* **303**:233-240.
- Shipkova M, Strassburg CP, Braun F, Grone HJ, Armstrong VW, Tukey RH, Ollerich M, and Wieland E (2001) Glucuronide and glucoside conjugation of mycophenolic acid by human liver, kidney and intestinal microsomes. *Br J Pharmacol* **132**:1027-1034.
- Stone AN, Mackenzie PI, Galetin, A, Houston JB, and Miners, JO (2003) Isoform selectivity and kinetics of morphine 3-and 6-glucuronidation by human UDP-glucuronosyltransferases: Evidence for atypical glucuronidation kinetics by UGT2B7. *Drug Metab Dispos* **31**:1086-1089.
- Tang BK (1990) Drug glucosidation. *Pharmacol Ther* **46**:53-56.

Tang CY, Hochman JH, Ma B, Subramanian R, and Vyas KP (2003) Acyl glucuronidation and glucosidation of a new and selective endothelin ETA receptor antagonist in human liver microsomes. *Drug Metab Dispos* **31**:37-45.

Toide K, Terauchi Y, Fujii T, Yamazaki H, and Kamataki T (2004) Uridine diphosphate sugar-selective conjugation of an aldose reductase inhibitor (AS-3201) by UDP-glucuronosyltransferase 2B subfamily in human liver microsomes. *Biochem Pharmacol* **67**:1269-1278.

Uchaipichat V, Mackenzie PI, Guo X-H, Gardner-Stephen D, Galetin A, Houston JB, and Miners JO (2004) Human UDP-glucuronosyltransferases: Isoform selectivity and kinetics of 4-methylumbelliferone and 1-naphthol glucuronidation, effects of organic solvents, and inhibition by diclofenac and probenecid. *Drug Metab Dispos* **32**:413-423.

Uchaipichat V, Winner LK, Mackenzie PI, Elliot DJ, Williams JA, and Miners JO (2006) Quantitative prediction of *in vivo* inhibitory interactions involving glucuronidated drugs from *in vitro* data: the effect of fluconazole on zidovudine glucuronidation. *Br J Clin Pharmacol* **61**:427-439.

Yang F, Machalz D, Wang S, Li Z, Wolber G, and Bureik M (2018) A common polymorphic variant of UGT1A5 displays increased activity due to optimized cofactor binding. *FEBS Lett* **592**:1837-1846.

Zhang H, Patana A-S, Mackenzie PI, Ikushiro S, Goldman A, and Finel M (2012) Human UDP-glucuronosyltransferase expression in insect cells: Ratio of active to inactive recombinant proteins and the effects of C-terminal His-tag on glucuronidation kinetics. *Drug Metab Dispos* **40**:1935-1944.

Zientek MA and Youdim K (2015), Reaction phenotyping: Advances in the experimental strategies used to characterize the contribution of drug-metabolizing enzymes', *Drug Metab Dispos* **43**:163-181.

FIGURE LEGENDS

Figure 1. Eadie-Hofstee plots for morphine 3-glucosidation by c-SUP (Panel A) and uninfected Sf9 membranes (Panel B). The substrate concentration range was 0.05 – 10 mM.

Figure 2. Glucosidation of xenobiotics containing either an aliphatic, phenolic hydroxyl, amine- or carboxyl- group at 4 substrate concentrations by uninfected Sf9 membranes and c-SUP: 21-OHPr (Panel A), 1-OHP (Panel B), 4-MU (Panel C), MPA (Panels D and I), 1-NAP (Panel E), 4-NP (Panel F), PE (Panel G), AZT (Panel H), S-NAP (Panel J), BZC (Panel K), LTG (Panel L) and TFP (Panel M). Bars represent the mean of duplicate measurements (<10% variance).

Figure 3. Eadie-Hofstee plots for 1-OHP (Panels A and B), MPA (Panels C and D), and 4-MU (Panels E and F) glucosidation by c-SUP and uninfected Sf9 membranes. Substrate concentration ranges: 1-OHP, 0.2 – 8 μ M; MPA, 10 – 600 μ M; and 4-MU, 5 – 1000 μ M.

Figure 4. Immunoblots of UGT1A5 expressed in HEK293T (Panel A), COS7 (Panel B) and Sf9 (Panel C) cells. Lane 1, wild-type UGT1A5; Lane 2, UGT1A5-His40Pro; Lane 3, UGT1A5-Thr36Ile; Lane 4, positive controls (UGT1A1 (panels A and B) and His-tagged CYP1A1 (panel C)); Lane 5, negative controls (untransfected HEK293T (panel A) and COS7 (panel B) cell lysate, and uninfected Sf9 (panel C) cell membranes). Immuno-reactive bands are observed at 55 kDa for UGT1A5 and its mutants, 58 kDa for CYP1A1 and 60 kDa for UGT1A1. Western blots were performed in duplicate.

Table 1. Observed and predicted m/z values (Da) of xenobiotic glucosides formed by incubations of uninfected Sf9 membranes and c-SUP with UDP-glucose as cofactor.

Xenobiotic	Predicted glucoside m/z	Observed glucoside m/z	
		Sf9 membranes	c-SUP
Benzocaine	328.13	328.13	328.13
Codeine	462.21	ND	ND
21-Hydroxyprogesterone	493.27	493.28	493.27
1-Hydroxypyrene	381.13	381.14	381.13
Lamotrigine	418.07	418.07	ND
4-Methylumbelliferone	339.10	339.08	339.09
Morphine	448.19	448.18	448.18
Mycophenolic acid (phenolic and acyl)	483.18	483.19	483.19
1-Naphthol	307.12	307.12	307.13
S-Naproxen	410.18 ^a	410.16 ^a	410.18 ^a
	415.13 ^b	415.13 ^b	415.11 ^b
	431.11 ^c	431.11 ^c	431.10 ^c
Phenethyl alcohol	285.13	285.15	285.13
Trifluoperazine	571.23	571.22	ND
Zidovudine	430.16	ND	431.16

^a S-naproxen + NH₄ adduct

^b S-naproxen + Na adduct

^c S-naproxen + K adduct

ND – not detected

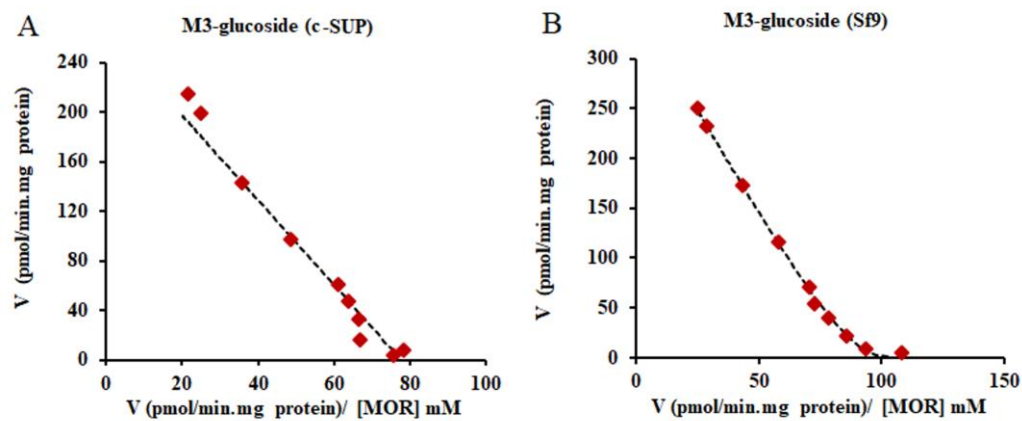


Figure 1

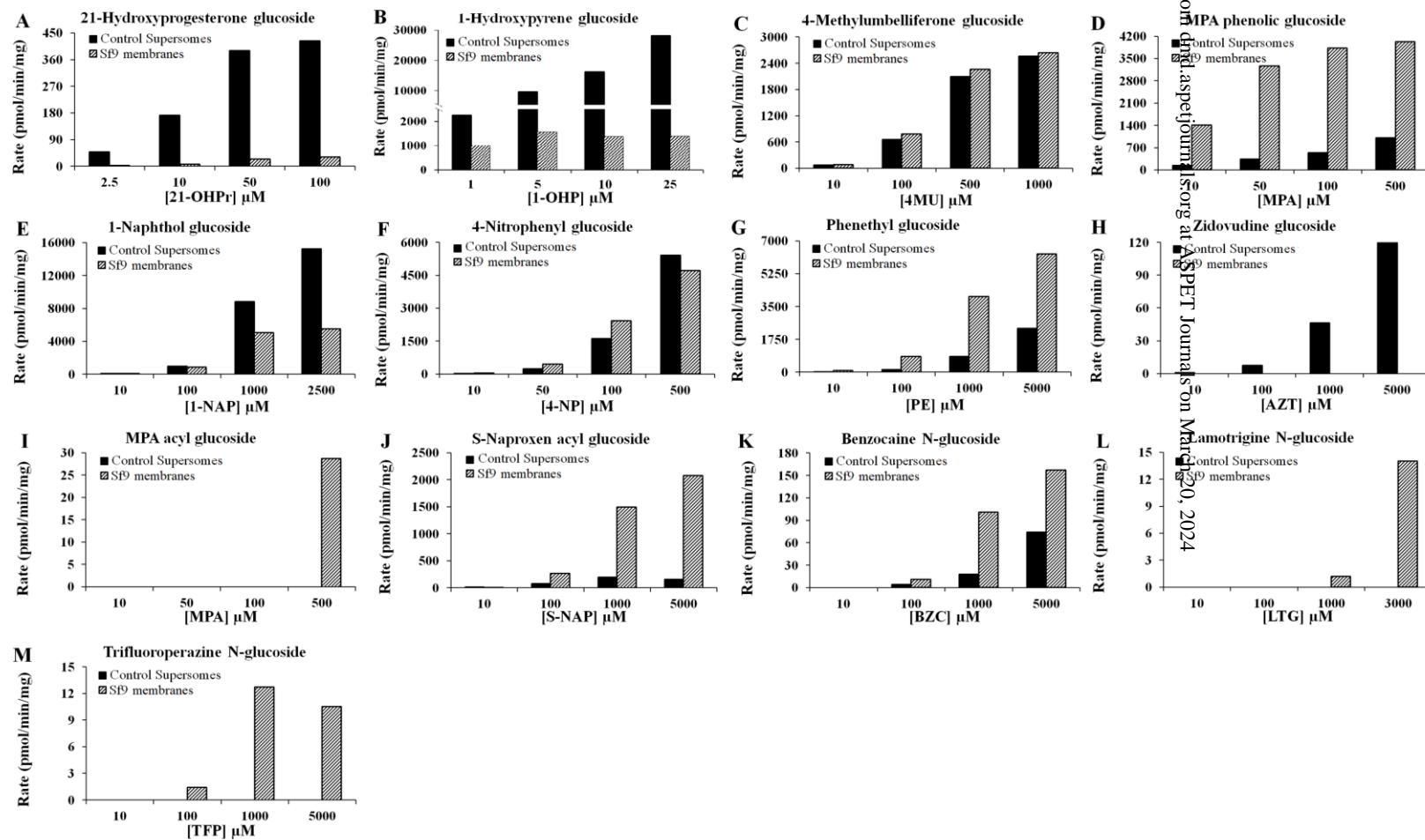


Figure 2

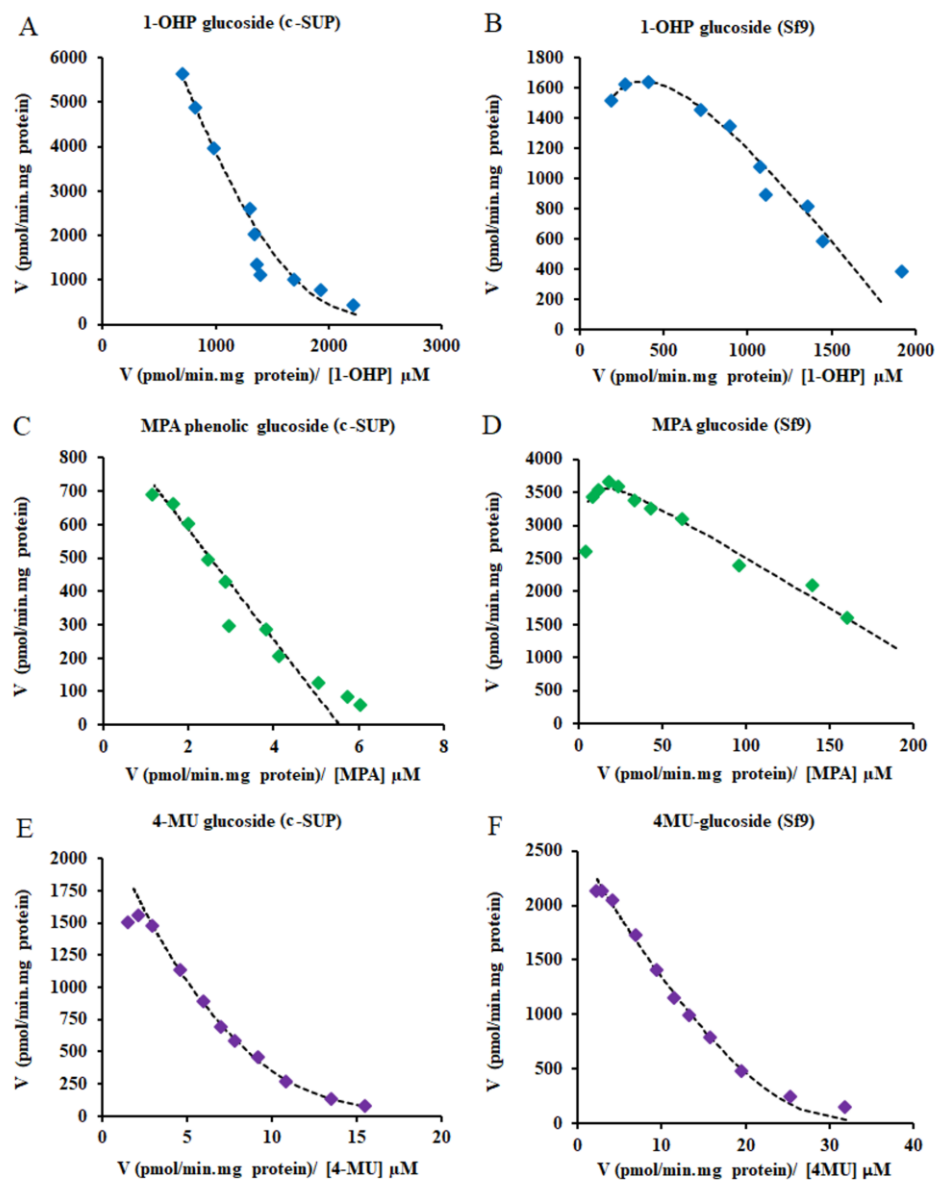


Figure 3

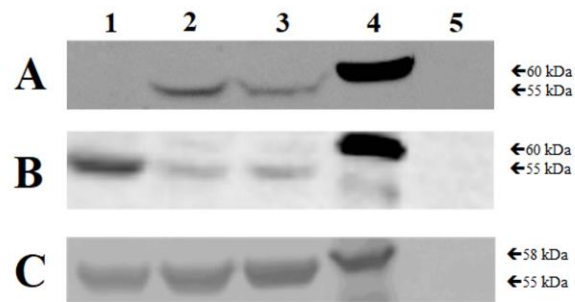


Figure 4

Supplemental data.

Drug and chemical glucosidation by control Supersomes and membranes from *Spodoptera frugiperda* (Sf) 9 cells: Implications for the apparent glucuronidation of xenobiotics by UDP-glucuronosyltransferase 1A5.

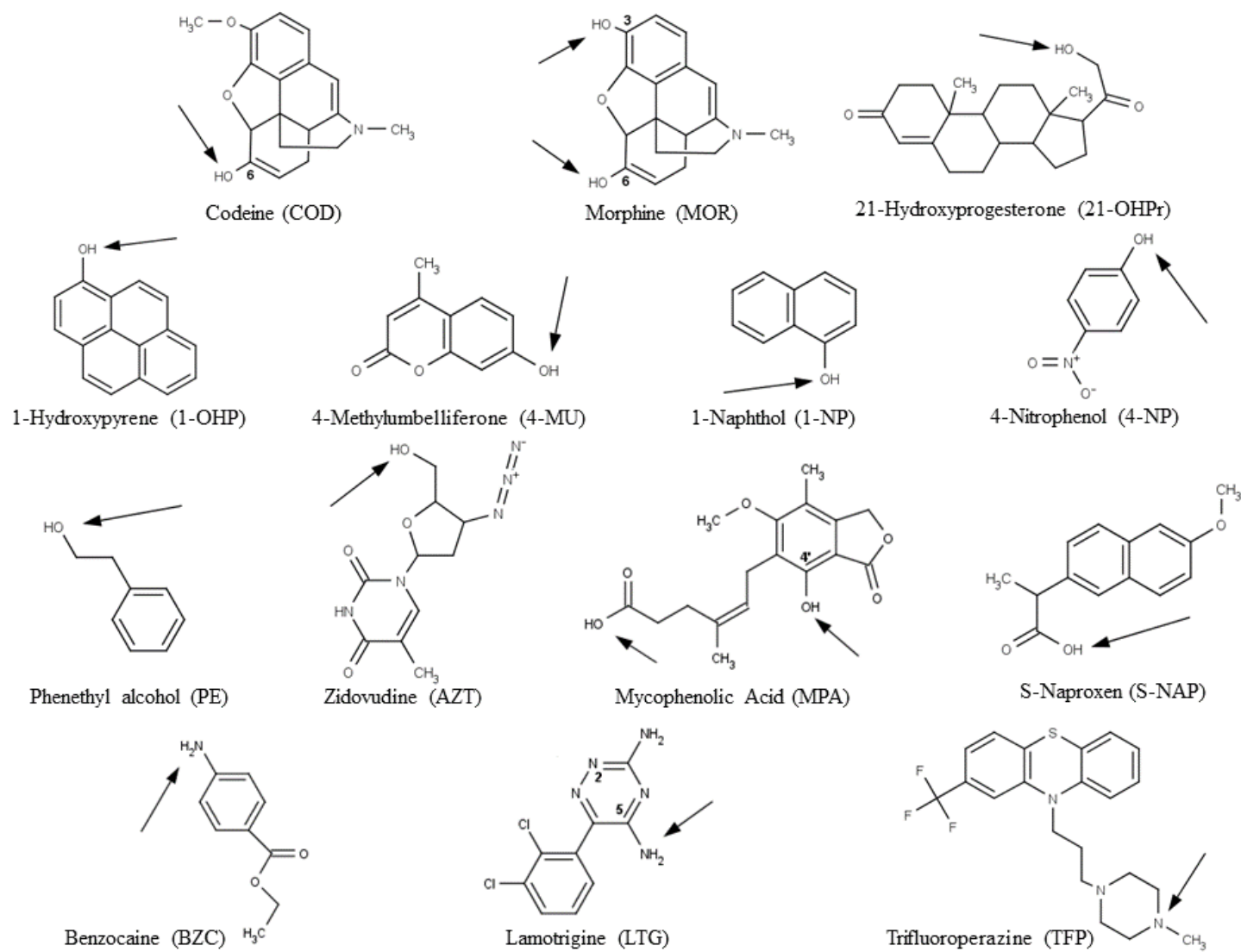
Nuy Chau, Leyla Kaya, Benjamin C. Lewis, Peter I. Mackenzie and John O. Miners.

Drug Metabolism and Disposition.

Legend to Supplemental Figure 1: Structures of agylcones. Arrows show the primary site(s) of glucosidation.

.

Supplemental Figure 1.



Supplemental Table 1. HPLC assay conditions (see text for aglycone abbreviations)

Substrate and glycoside conjugate	Retention time (min)	Mobile phase A ^a	Mobile phase B ^a	Protein precipitant (200μl incubation)	Calibration slope (compound) and range, μM)	Detection method ^b	Wavelength (nm)	HPLC Column	Injection volume (μl)
MOR	13.6	4mM 1-OSA, 5% ACN, 1% glacial AcOH in water, pH 2.6	ACN					C18 Waters Nova-Pak 4μm (3.9×150mm) with guard column	10
M3-glucoside ^c	8.5	96% - 0 min 91% - 10 min 91% - 11 min 75% - 11.1 min 75% - 11.9 min 96% - 12 min 96% - 20min	4% - 0 min 9% - 10 min 9% - 11 min 25% - 11.1 min 25% - 11.9 min 4% - 12 min 4% - 20min	2μL HClO ₄ (70%)	4.24 (M3-glucoside) (2-80)	FL	(λ _{ex}) 235 (λ _{em}) 345		with needle wash injection (50/50 ACN/water)
MPA	6.8	10mM ammonium acetate, pH 5.7 (glacial AcOH), 10% ACN in water	ACN					C18 Waters Nova-Pak 4μm (3.9×150mm) with guard column	20
MPA-glucoside ^c	4.5	95% - 0 min 95% - 1 min 40% - 11 min 95% - 11.1 min	5% - 0 min 5% - 1 min 60% - 11 min 5% - 11.1 min	2μL HClO ₄ (70%)	9.99 (MPA-glucoside) (2.5-25)	UV	250		with needle wash injection (50/50 ACN/water)
AcMPA-glucoside ^c	7.4								
4MU	5.8	10mM TEA, pH 2.5 (HClO ₄), 10% ACN in water	ACN					C18 Waters Nova-Pak 4μm (3.9×150mm)	40
4MUG-glucoside ^c	3.35	96% - 0 min 96% - 3 min 70% - 3.1 min 70% - 4.1 min 96% - 4.2 min	4% - 0 min 4% - 3 min 30% - 3.1 min 30% - 4.1 min 4% - 4.2 min	2μL HClO ₄ (70%)	29.45 (4MU-glucoside) (1-20)	UV	316		
TFP	9.95	0.1% TFA in water	0.1% TFA in ACN					Beckman ODS 5μm (4.6×250mm)	40
TFPG-glucuronide ^d	8.99	69% - 0 min 52% - 9 min 69% - 9.1 min	31% - 0 min 48% - 9 min 31% - 9.1 min	200μL 4% AcOH in MeOH	35.3 (TFP) (1-10)	UV	256		
TFP-glucoside ^d	8.73								

Substrate and glycoside conjugate	Retention time (min)	Mobile phase A ^a	Mobile phase B ^a	Protein precipitant (200μl incubation)	Calibration slope (compound) and range, μM)	Detection method ^b	Wavelength (nm)	HPLC Column	Injection volume (μl)
LTG	10.85	25mM phosphate buffer pH 7.4: ACN: TEA (95:5:0.02)	ACN						
LTG-N2-glucuronide ^c	4.68	96% - 0 min 96% - 3 min 87% - 7 min 87% - 8 min 50% - 9 min 50% - 11 min 96% - 14 min	96% - 0 min 96% - 3 min 87% - 7 min 87% - 8 min 50% - 9 min 50% - 11 min 96% - 14 min	2μl HClO ₄ (11.6 M)	10.5 (LTG-N2-glucuronide) (2.5-10)	UV	254	Zorbax Eclipse XDB-C8 5μm (4.6×150mm)	20
LTG-glucoside ^d	9.32								
COD	4.49	2mM TEA pH 2.7 (HClO ₄), 10% ACN	ACN						
COD-6-glucuronide ^c	3.32	100% - 0 min 100% - 5.5 min 40% - 5.6 min 40% - 6.4 min 100% - 6.5 min 100% - 15 min	0% - 0 min 0% - 5.5 min 60% - 5.6 min 60% - 6.4 min 0% - 6.5 min 0% - 15 min	2μl HClO ₄ (11.6 M)	5.18 (COD-6-glucuronide) (2.5-10)	UV	205	Phenomenex Synergi HydroRP C18 4μm (3.9×150mm)	5
COD-6-Glc ^d	ND								
S-NAP	10.52								
S-NAP-glucuronide ^d	2.75	0.12% AcOH in water, 30% ACN ^e		200μl 4% AcOH in MeOH	34.6 (S-NAP) (0.5-25)	UV	225	C18 Waters Nova-Pak 4μm (3.9×150mm)	30
S-NAP-glucoside ^d	2.68								
AZT	6.16	10mM TEA, pH 2.5 (HClO ₄)	ACN						
AZT-glucuronide ^c	4.24	95% - 0 min 95% - 3 min 90% - 6 min 90% - 8 min 95% - 8.1 min	5% - 0 min 5% - 3 min 10% - 6 min 10% - 8 min 5% - 8.1 min	2μl HClO ₄ (11.6 M)	6.7 (AZT-glucuronide) (2.5-20)	UV	267	C18 Waters Nova-Pak 4μm (3.9×150mm)	15
AZT-glucoside ^d	3.41								

Substrate and glycoside conjugate	Retention time (min)	Mobile phase A ^a	Mobile phase B ^a	Protein precipitant (200μl incubation)	Calibration slope (compound) and range, μM)	Detection method ^b	Wavelength (nm)	HPLC Column	Injection volume (μl)
1-NAP	6.5-	10mM TEA, pH 2.5 (HClO ₄), 10% ACN in water	ACN		5.54			C18	
1-NAP-glucuronide ^c	4.67	86% - 0 min 86% - 4 min 36% - 4.1 min	14% - 0 min 14% - 4 min 64% - 4.1 min	2μl HClO ₄ (11.6 M)	(1-NAP-glucuronide)	UV	90	Waters Nova-Pak 4μm (3.9×150mm)	20
1-NAP-glucoside ^d	3.80	36% - 5 min 86% - 5.1 min	64% - 5 min 14% - 5.1 min		(5-80)				
4-NP	10.80	10mM ammonium acetate in water, pH 5.7 (glacial AcOH)	ACN		2.78			C18	
4-NPG-glucoside ^c	3.85	90% - 0 min 90% - 2 min 80% - 10 min 90% - 12 min	10% - 0 min 10% - 2 min 20% - 10 min 10% - 12 min	2μl HClO ₄ (11.6 M)	(4-NP-glucoside)	UV	302	Waters Nova-Pak 4μm (3.9×150mm)	5
					(2-100)				
PE	8.05	10mM ammonium acetate in water, pH 5.7 (glacial AcOH)	ACN		2.59			C18	
PE-glucoside ^c	5.20	87.5% - 0 min 87.5% - 2 min 75% - 10 min 87.5% - 10.1 min	17.5% - 0 min 17.5% - 2 min 25% - 10 min 17.5% - 10.1 min	2μl HClO ₄ (11.6 M)	(PE-glucoside)	UV	215	Waters Nova-Pak 4μm (3.9×150mm)	10
					(10-100)				
21-OHPr	10.45	10mM ammonium acetate in water, pH 5.7 (glacial AcOH)	ACN		5.27			C18	
21-OHPr-glucoside ^c	6.30	75% - 0 min 75% - 2 min 50% - 10 min 75% - 10.1 min	25% - 0 min 25% - 2 min 50% - 10 min 25% - 10.1 min	2μl HClO ₄ (11.6 M)	(21-OHPr-glucoside)	UV	248	Waters Nova-Pak 4μm (3.9×150mm)	20
					(2.5-100)				

Substrate and glycoside conjugate	Retention time (min)	Mobile phase A ^a	Mobile phase B ^a	Protein precipitant (200μl incubation)	Calibration slope (compound) and range, μM)	Detection method ^b	Wavelength (nm)	HPLC Column	Injection volume (μl)
1-OHP	9.95	1% formic acid, 5% ACN in water, pH 2.1	ACN	200μl	297 (1-OHP-glucuronide)	FL	(λ _{ex}) 242 (λ _{em}) 382	C18 Waters Nova-Pak 4μm (3.9×150mm)	5
1-OHP-glucoside ^d	5.65	77.5% - 0 min 77.5% - 2 min 70% - 2.1 min 70% - 7.5 min 10% - 7.6min 10% - 9 min 77.5% - 9.1min 77.5% - 12 min	22.5% - 0 min 22.5% - 2 min 30% - 2.1 min 30% - 7.5 min 90% - 7.6min 90% - 9 min 22.5% - 9.1min 22.5% - 12 min	4% AcOH in MeOH	(1-20)				
BZC	10.15	10mM ammonium acetate in water, pH 5.7 (glacial AcOH)	ACN	200μl	5.55 (BZC-glucoside)	UV	291	C18 Waters Nova-Pak 4μm (3.9×150mm)	10
BZC-glucoside ^c	3.69	85% - 0 min 85% - 2 min 70% - 10 min 85% - 15 min	15% - 0 min 15% - 2 min 30% - 10 min 15% - 15 min	2% Ascorbic acid in MeOH	(2-100)				

^a Abbreviations: ACN, acetonitrile; AcOH, acetic acid; HClO₄, perchloric acid; MeOH, methanol; OSA, octane sulfonic acid; TEA, triethylamine

^b FL, fluorescence detection; UV, ultraviolet detection

^c Calibration standard available commercially or synthesized in-house (morphine 3-glucoside)

^d Calibration standard not available commercially; glucoside conjugate identified from incubations performed with and without UDP-glucose and by UPLC-MS

ND, not detected